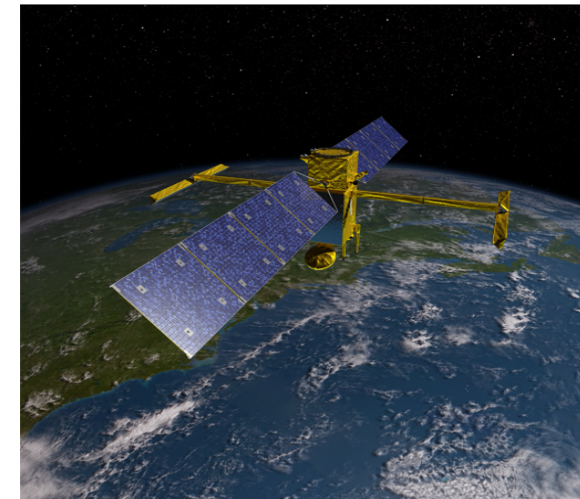


“Wave-Turbulence Interactions in the Oceans”

Patrice Klein (Caltech/JPL/Ifremer)

(VI) Stratified and Rotating Fluids



NEAR-INERTIAL WAVES AND TIDES:

- HAVE SIMILAR POWER INPUT ON A GLOBAL SCALE;
- SAME POTENTIAL TO CONTRIBUTE TO MIXING;
- CAN PROPAGATE FAR FROM THEIR SOURCES

NEAR-INERTIAL AND TIDAL WAVES EXPLAIN
A LARGE PART OF THE WAVE SPECTRUM
(~ 60 – 70%)

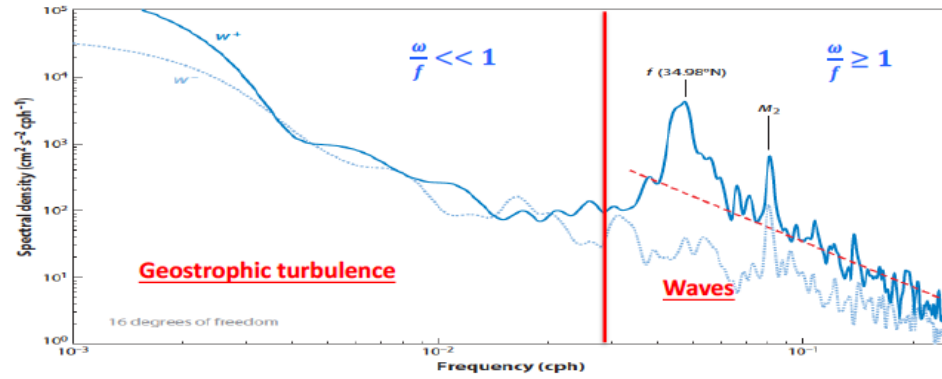


Figure 1

Rotary velocity spectrum at 261-m depth from current-meter data from the WHOI699 mooring gathered during the WESTPAC1 experiment (mooring at 6,149-m depth). The solid blue line (w^+) is clockwise motion, and the dashed blue line (w^-) is counterclockwise motion; the differences between these emphasize the downward energy propagation that often dominates the near-inertial band. The dashed red line is the line $E_0 N \omega^{-p}$ with $N = 2.0$ cycles per hour (cph), $E_0 = 0.096 \text{ cm}^2 \text{ s}^{-2} \text{ cph}^{-2}$, and $p = 2.25$, which is quantitatively similar to levels in the Cartesian spectra presented by Fu (1981) for station 5 of the Polygon Mid-Ocean Experiment (POLYMODE) II array.

NEAR-INERTIAL WAVES, MOSTLY WIND-DRIVEN (NEAR THE SURFACE) (TYPHOONS, CYCLONE),
ARE **INTERMITTENT AND WITH A STRONG SEASONALITY. THEY ARE AT LARGE SCALE.**

TIDAL WAVES **ARE FORCED GRAVITY WAVES**. INTERNAL TIDAL MOTIONS RESULT FROM THE
INTERACTION OF BAROTROPIC TIDES WITH THE TOPOGRAPHY. TIDAL WAVES HAVE **NO
SEASONALITY, NO INTERMITTENCY**. TYPICAL WAVELENGTHS ARE 100-150 KM.

GLOBAL DISTRIBUTIONS OF NEAR-INERTIAL WAVES AND TIDAL WAVES MUCH DIFFER.

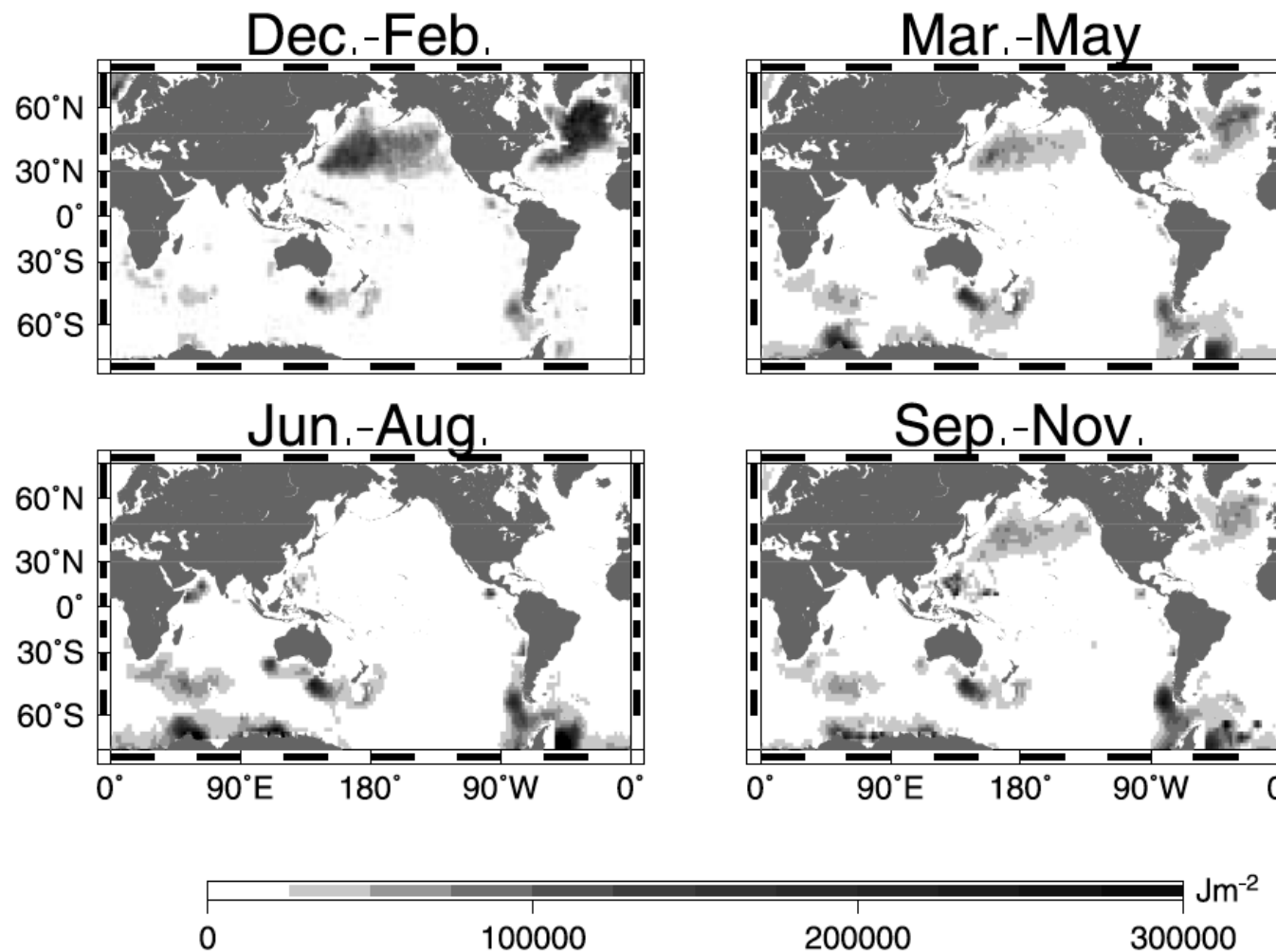


Figure 1. The global distribution of the wind-induced inertial energy input per unit ocean surface area during three months for each season which is averaged over 7 years from 1989 through 1995. The damping time r^{-1} is 4 days and the mixed layer thickness is kept constant at 50 m all over the world ocean.

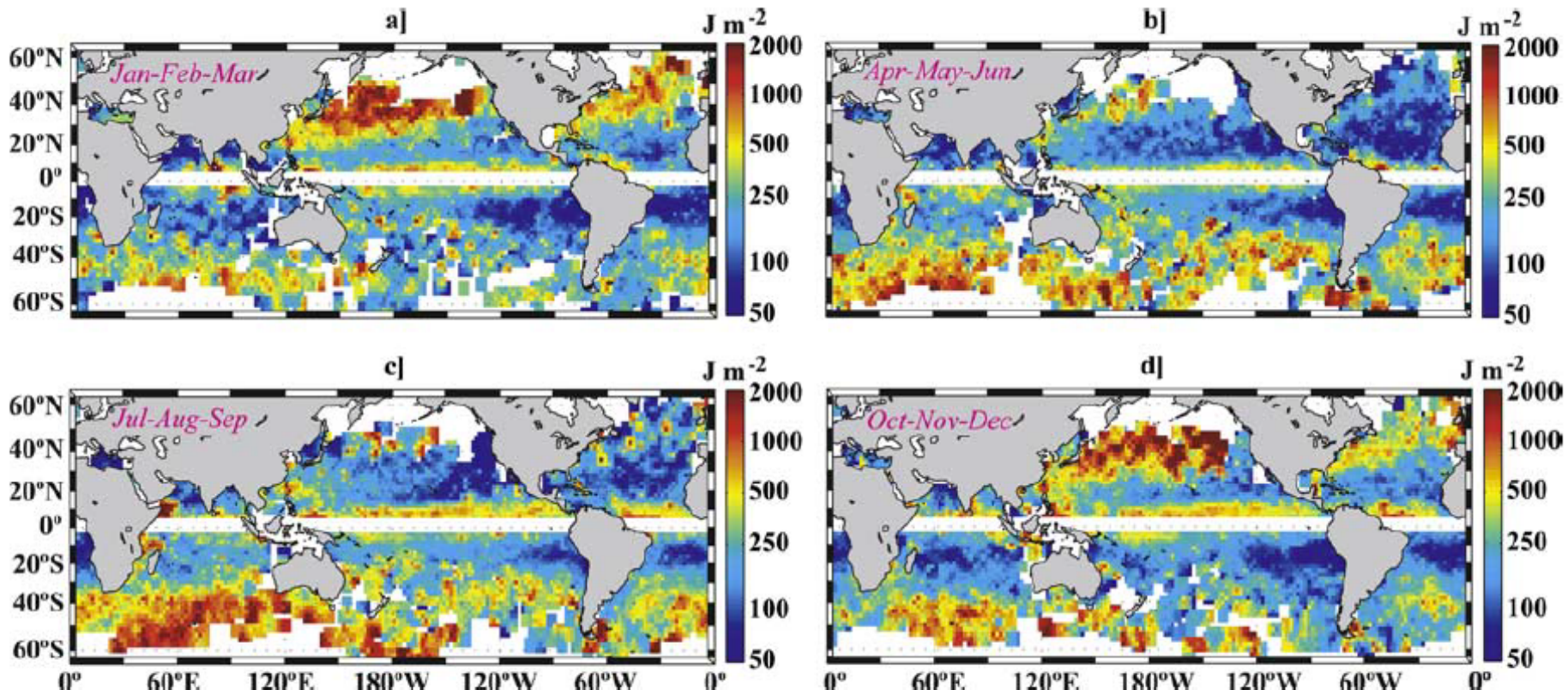
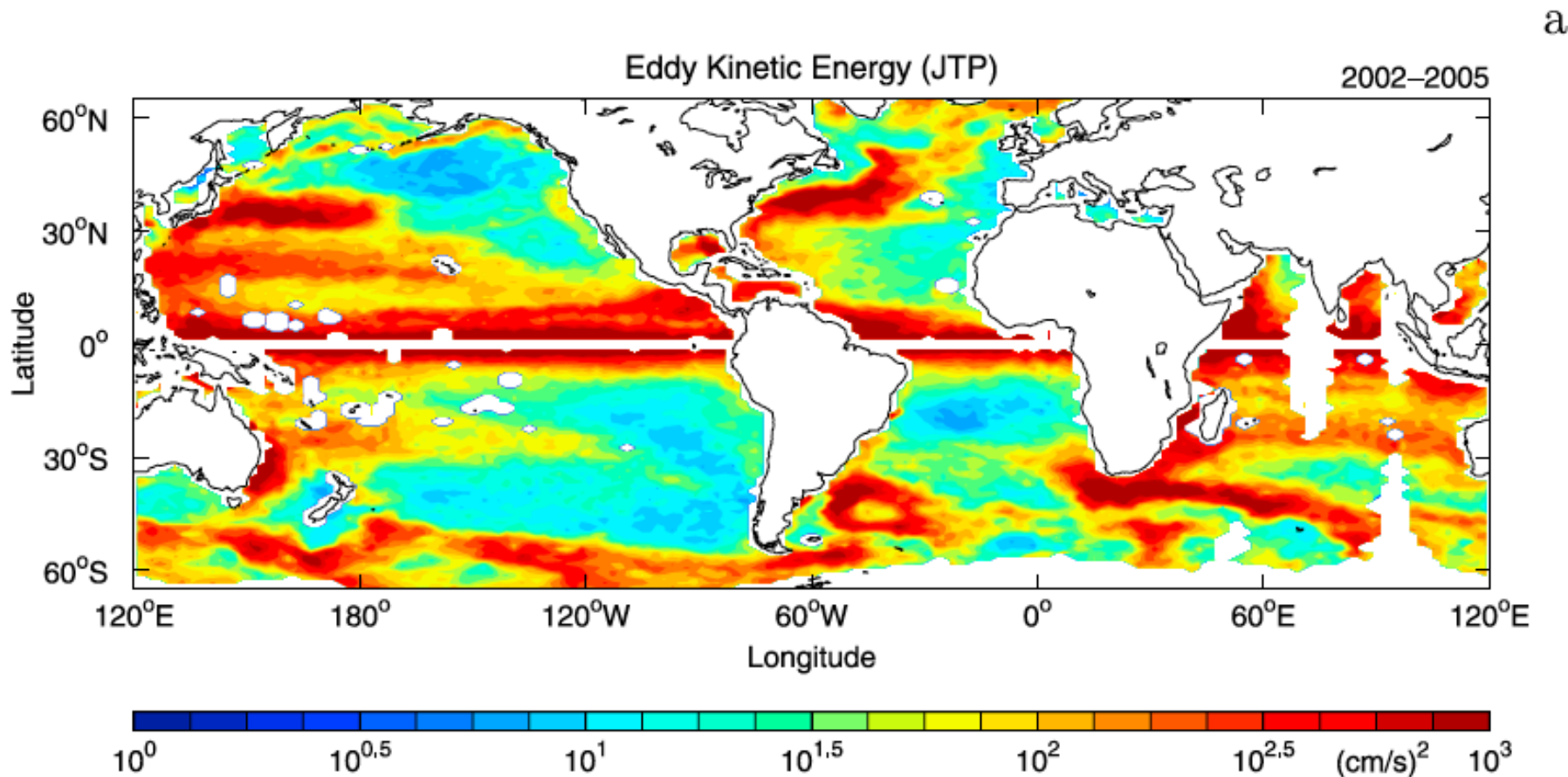


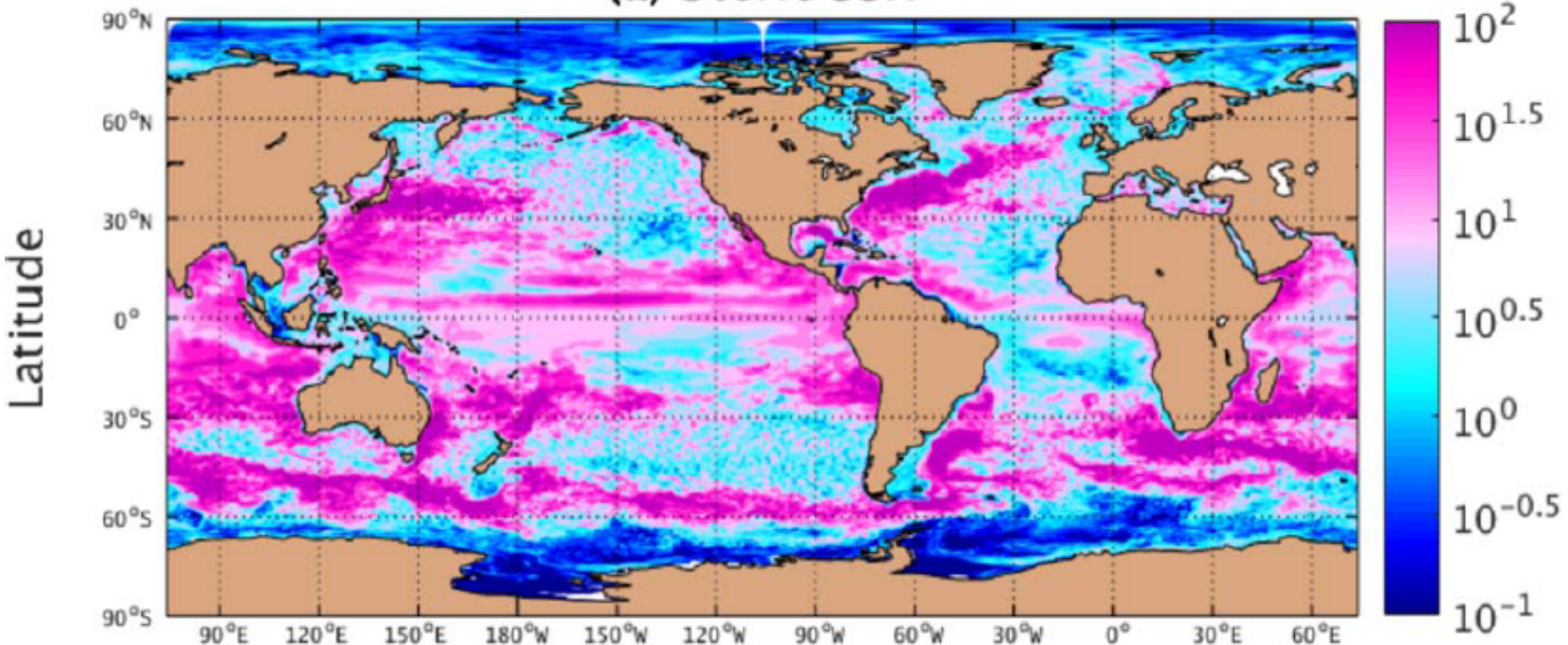
Figure 2. Seasonal variation of inertial mixed-layer energy computed from satellite-tracked drifter trajectories.

Chaigneau et al. GRL'08

Scharffenberg & Stammer JGR 2010: Using T/P & Jason 1 mission data

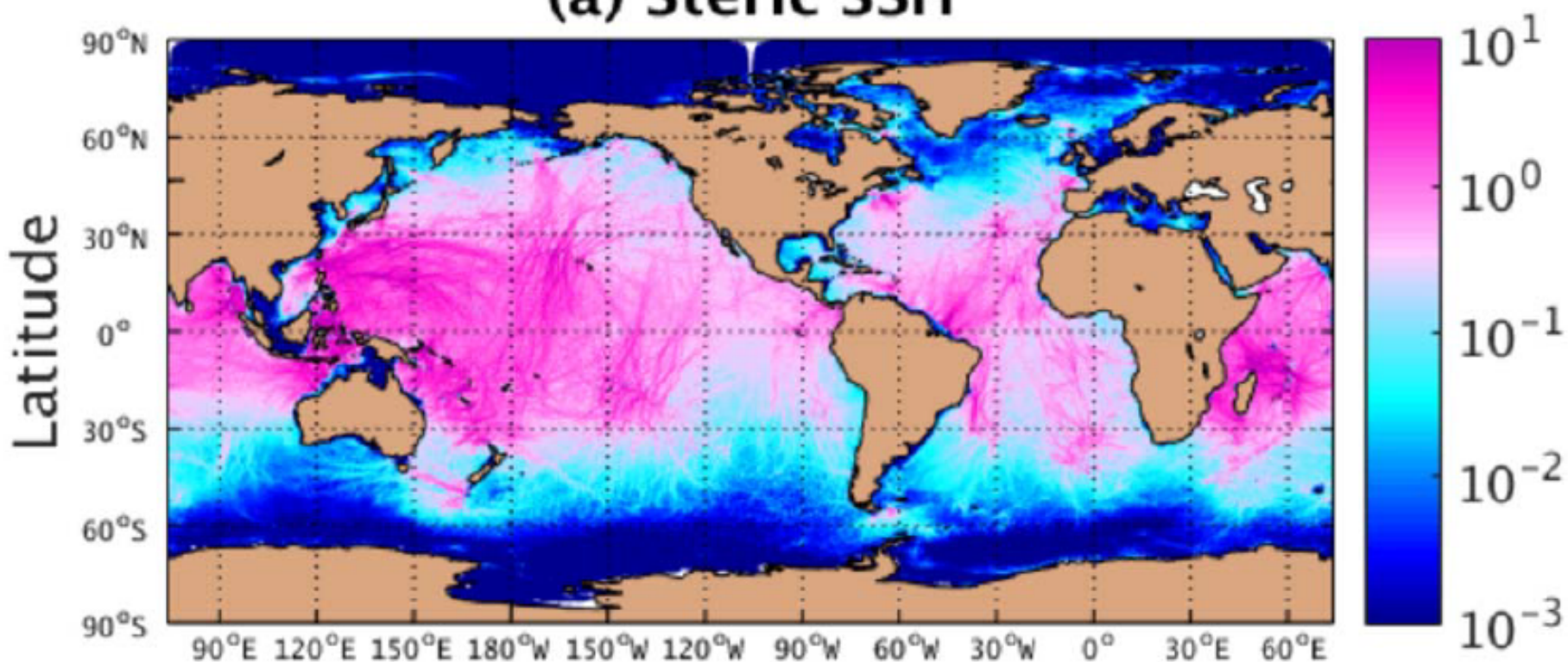


Subtidal
(a) Steric SSH



IMPACT OF MESOSCALE TURBULENCE ON THE SSH IN THE GLOBAL OCEAN
[GLOBAL SSH VARIANCE IN CM 2]

Semidiurnal (a) Steric SSH



IMPACT OF THE INTERNAL (M2) TIDE ON THE SSH IN THE GLOBAL OCEAN
[GLOBAL SSH VARIANCE IN CM²]

HF internal gravity waves (not only internal tides) have
an impact on SSH !

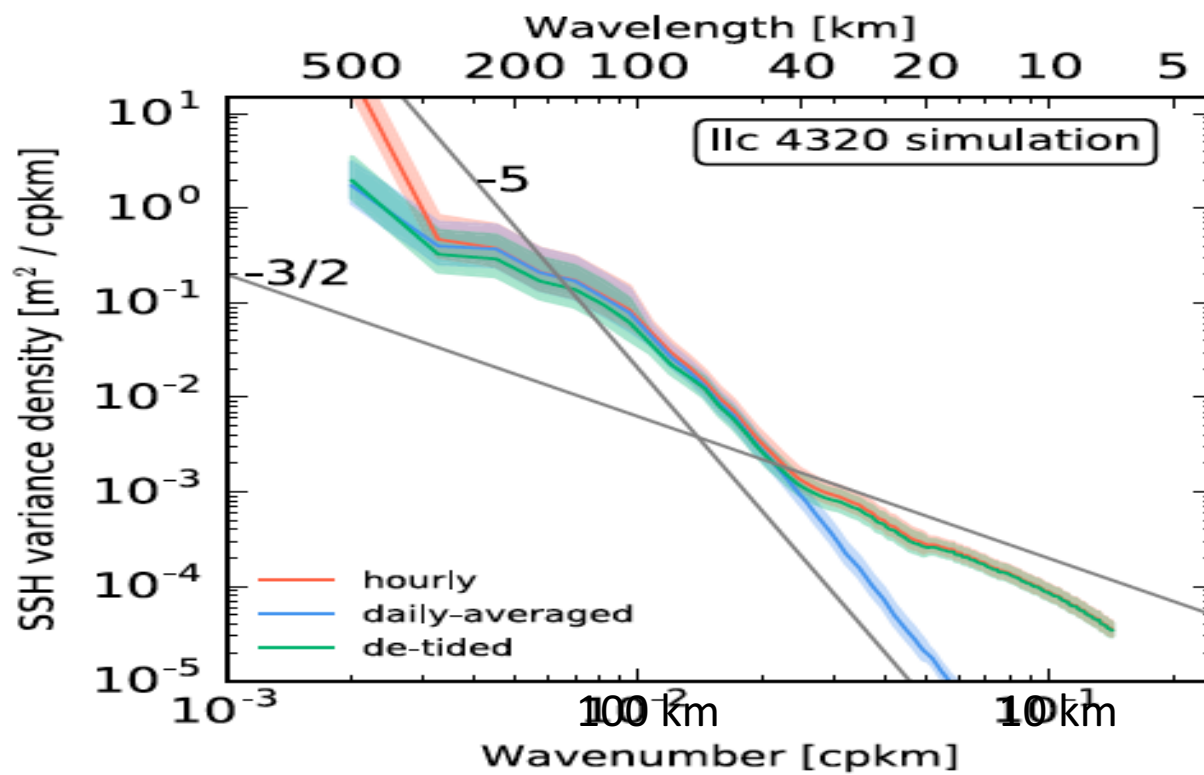
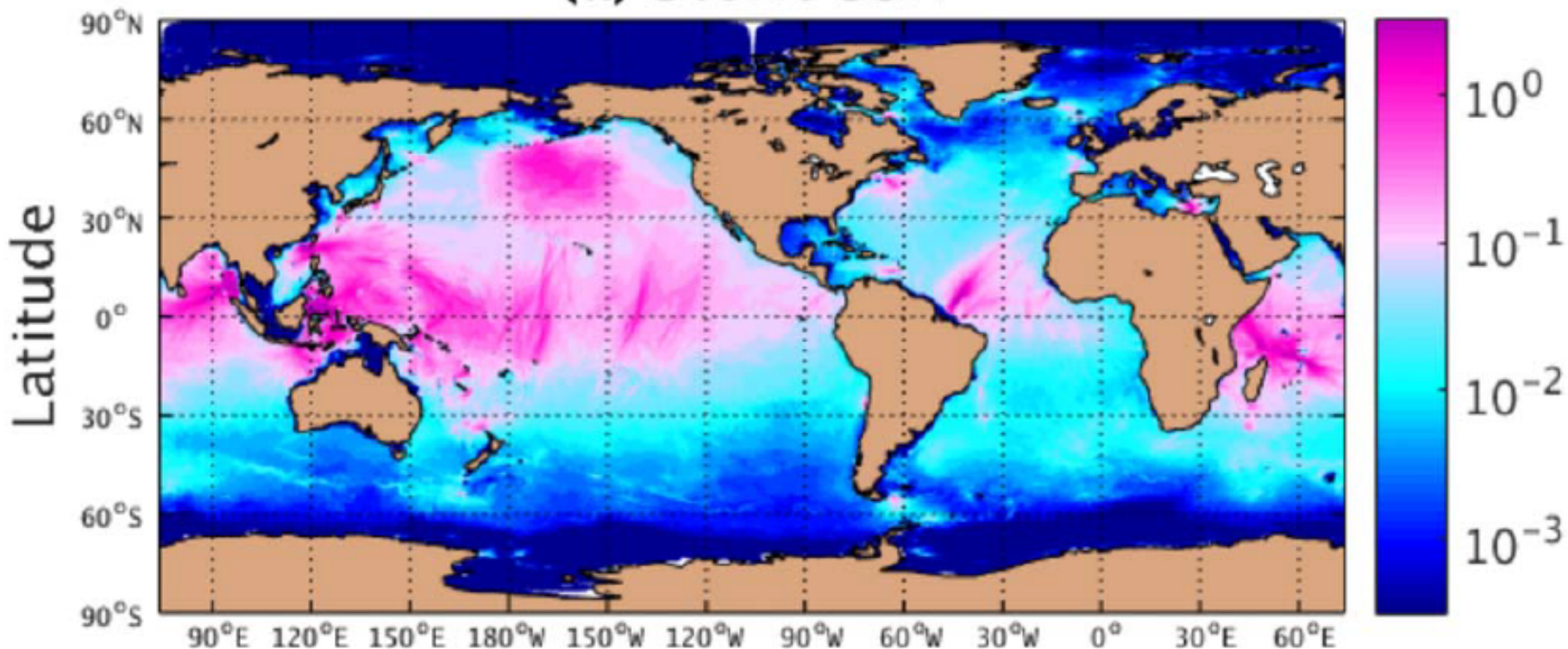


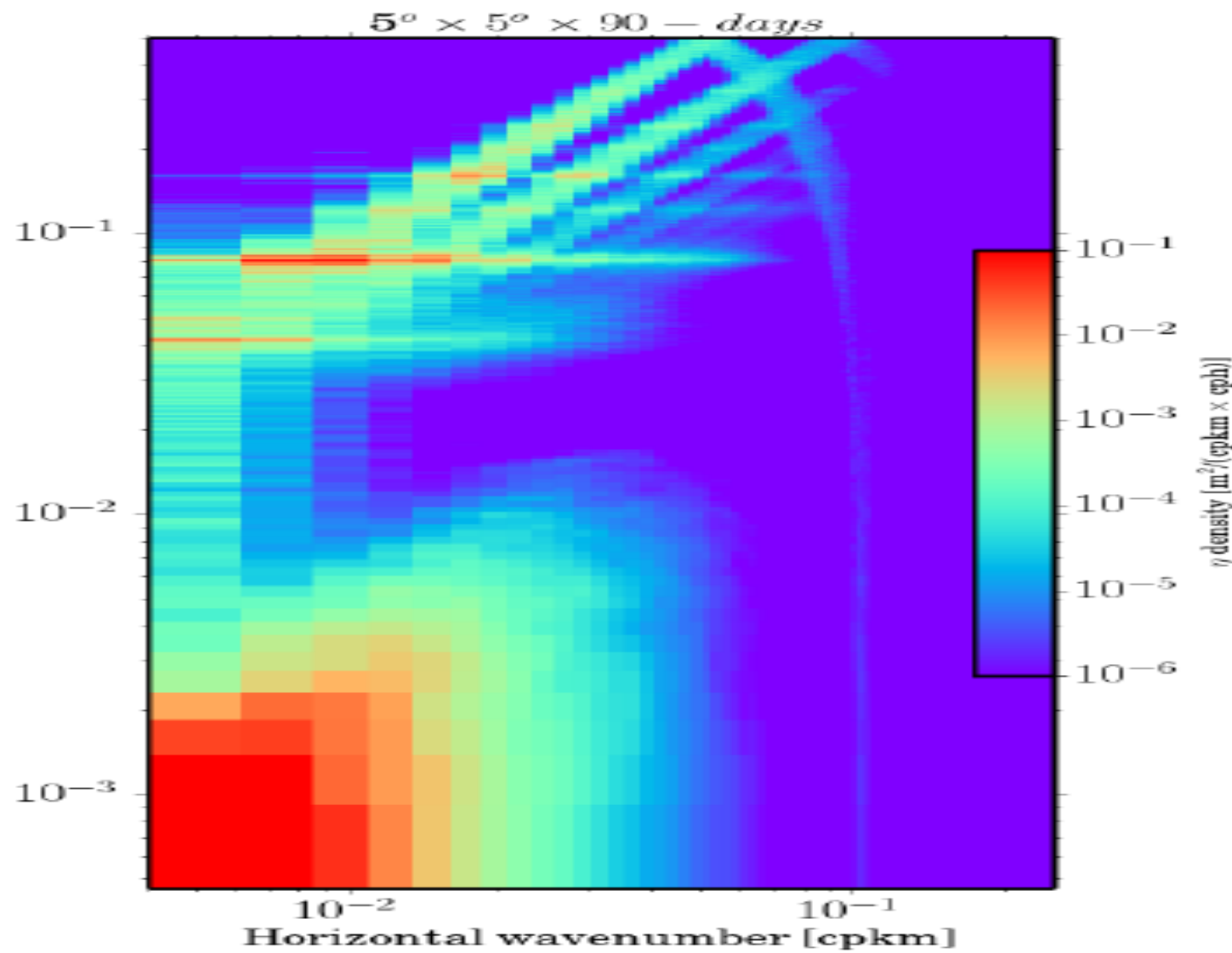
FIG. 9. Isotropic wavenumber SSH variance spectrum. Shaded regions represent 95% confidence limits. For reference, $k^{-3/2}$ and k^{-5} curves are plotted (gray lines).

Rocha et al. JPO 2016: in the Drake passage ...

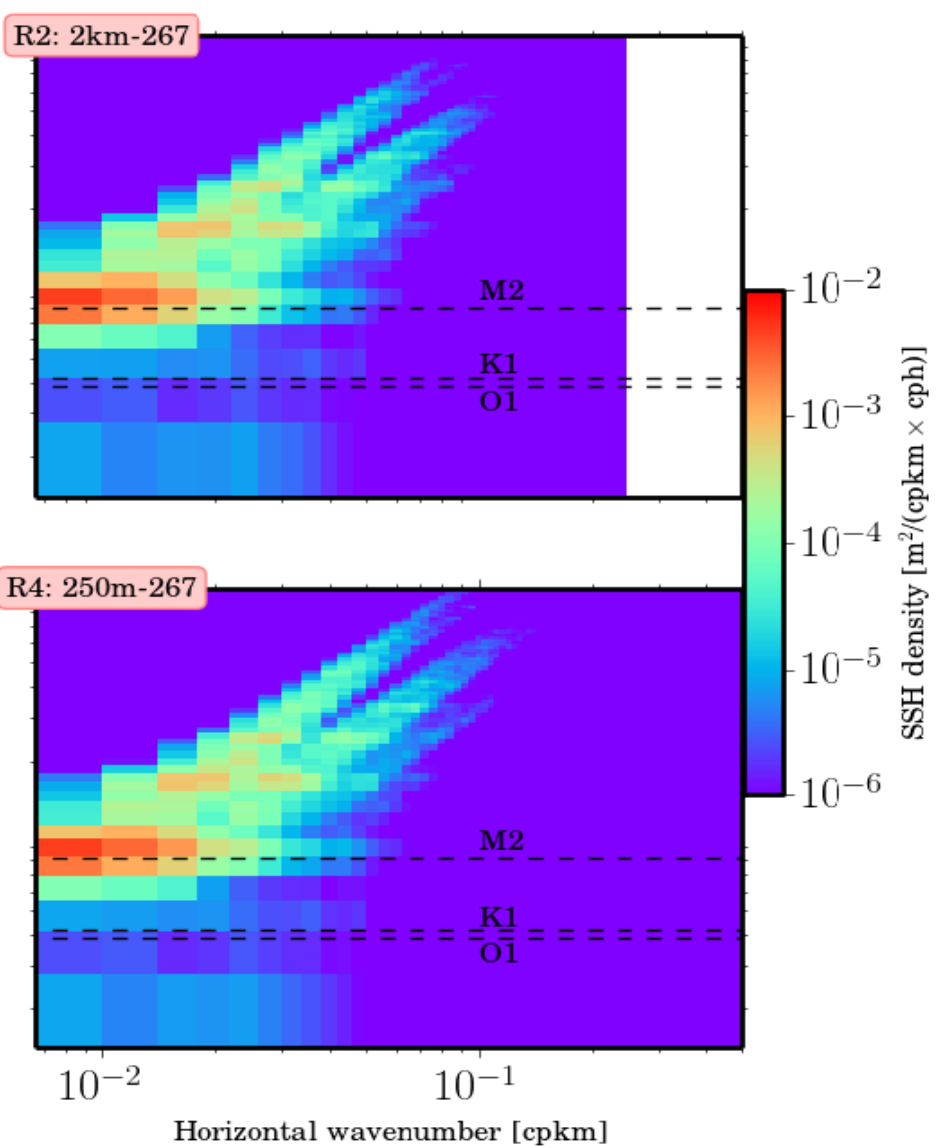
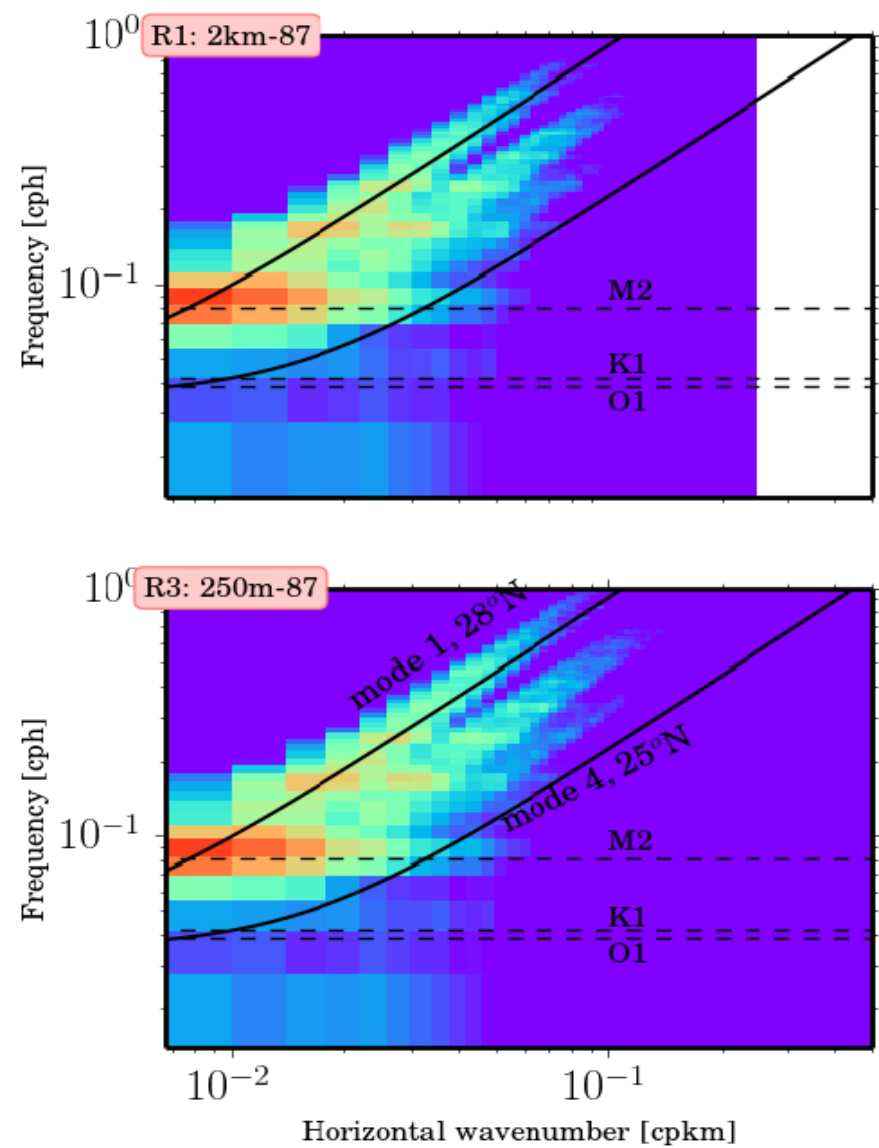
Supertidal (a) Steric SSH



IMPACT THE HIGHER-FREQUENCY INTERNAL WAVES ON THE SSH IN THE GLOBAL OCEAN
[GLOBAL SSH VARIANCE IN CM²]



Internal waves with frequencies higher than M2 frequency impact the ocean dynamics (SSH)
Rocha et al. JPO'16



The high frequency part of the wave spectrum is characterized by discrete bands!

THIS W-K SPECTRUM IS QUITE DIFFERENT WHEN TIDES ARE NOT PRESENT!

Dynamical fields display a strong seasonality!

Impacts the waves ($\omega > f$)

Square of the relative vorticity:

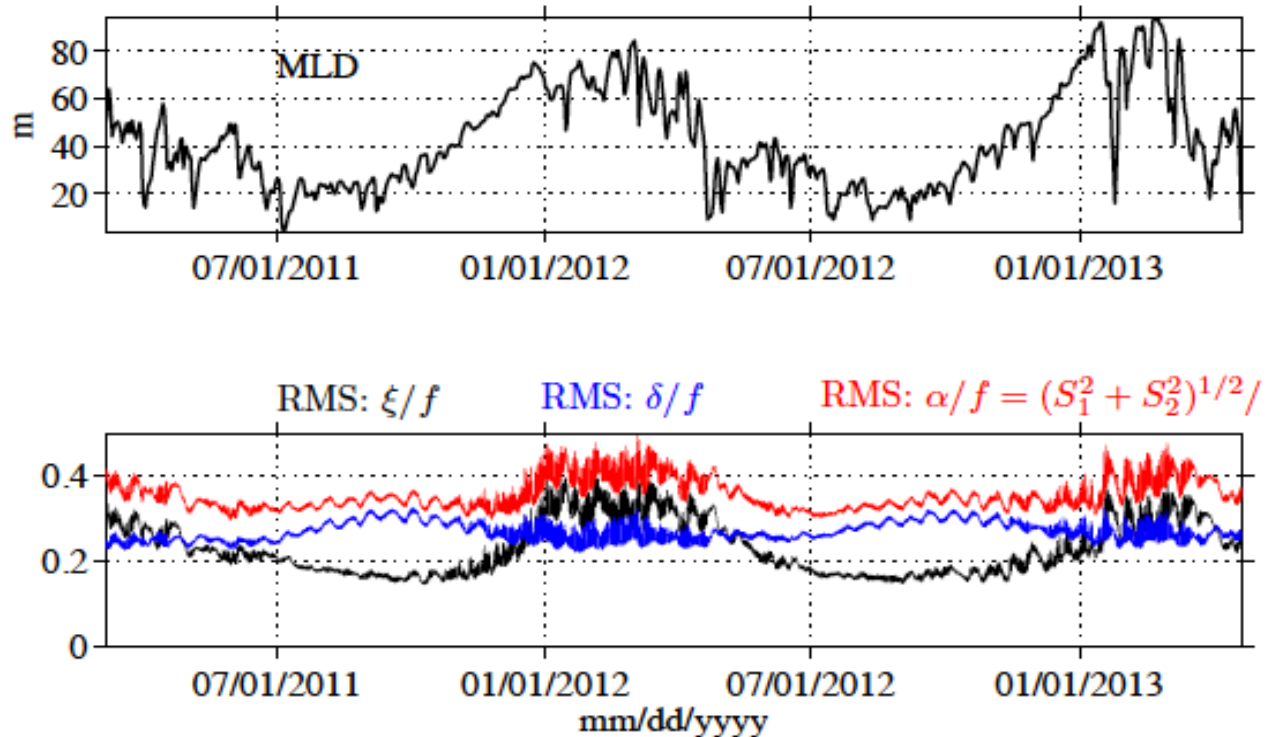
$$\xi^2 = \left(\frac{\partial v}{\partial x} - \frac{\partial u}{\partial y} \right)^2$$

Square of the horizontal flow divergence:

$$\delta^2 = \left(\frac{\partial u}{\partial x} + \frac{\partial v}{\partial y} \right)^2$$

Square of the horizontal strain:

$$S^2 = S_1^2 + S_2^2 = \\ \left(\frac{\partial u}{\partial x} - \frac{\partial v}{\partial y} \right)^2 + \left(\frac{\partial v}{\partial x} + \frac{\partial u}{\partial y} \right)^2$$



Relative vorticity is larger in winter (0.4) and divergence larger in summer (0.3)!

Seasonality is different with the wave part is removed!

and kinematic properties: daily-averaged

Square of the relative vorticity:

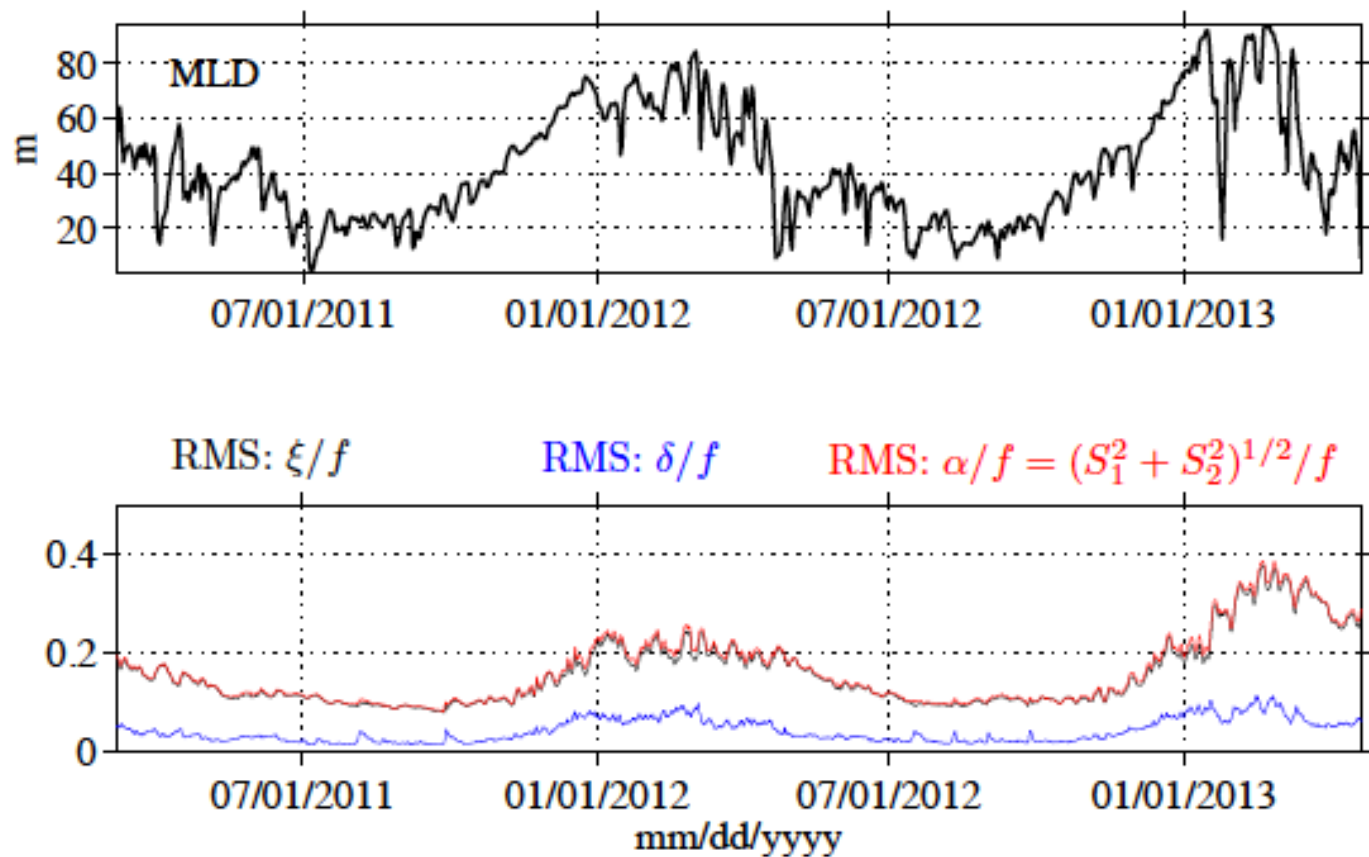
$$\xi^2 = \left(\frac{\partial v}{\partial x} - \frac{\partial u}{\partial y} \right)^2$$

Square of the horizontal flow divergence:

$$\delta^2 = \left(\frac{\partial u}{\partial x} + \frac{\partial v}{\partial y} \right)^2$$

Square of the horizontal strain:

$$S^2 = S_1^2 + S_2^2 = \left(\frac{\partial u}{\partial x} - \frac{\partial v}{\partial y} \right)^2 + \left(\frac{\partial v}{\partial x} + \frac{\partial u}{\partial y} \right)^2$$



Kuroshio Extension [Rocha et al. GRL 2016]

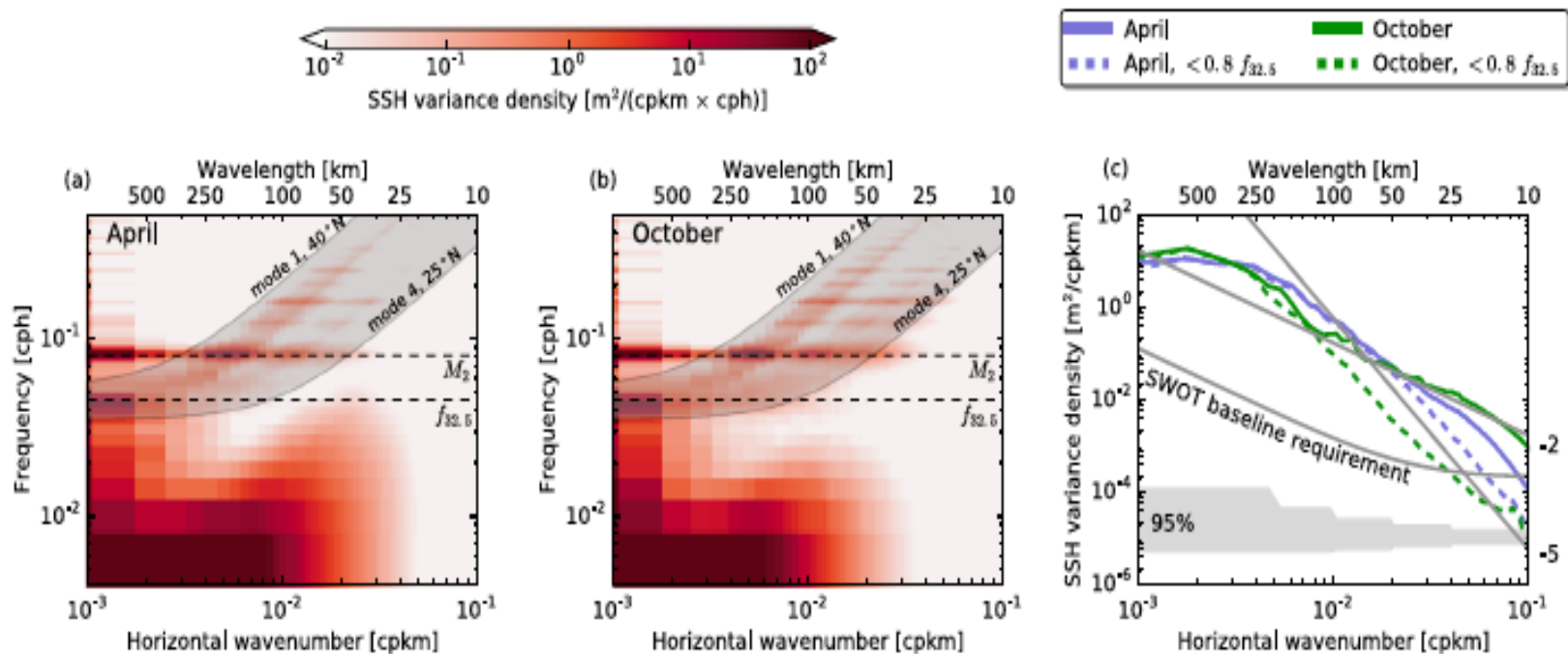
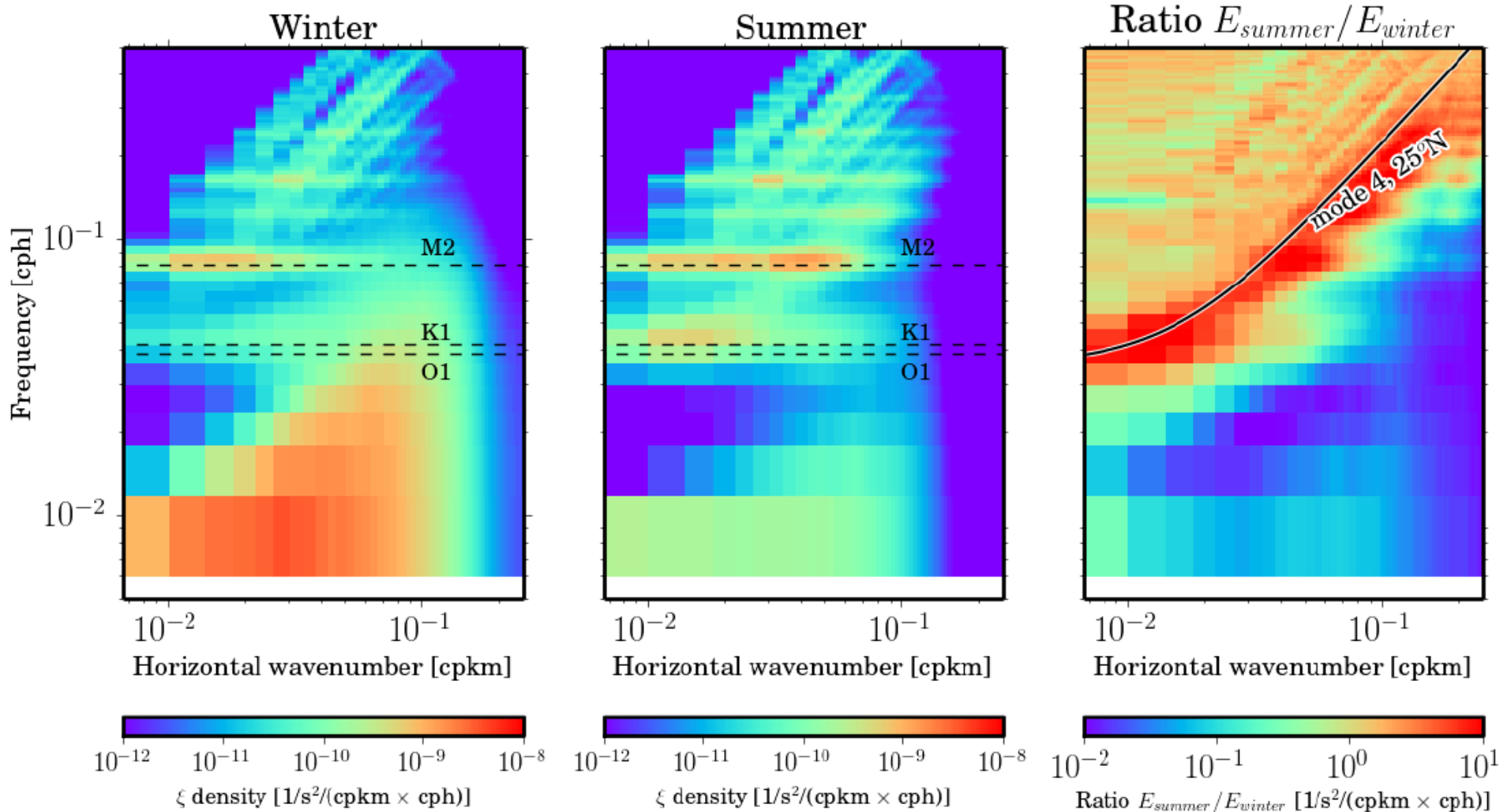


Figure 4. LLC4320 wave number-frequency spectrum of SSH variance in (a) April and (b) October. (c) Wave number spectrum of SSH variance—the integral of Figures 4a and 4b over frequency. In Figures 4a and 4b, the light gray shaded region depicts the dispersion relations for inertia-gravity waves from mode 1 through mode 4 across the latitudinal

- Both, internal tides and higher frequency internal gravity waves impact SSH;
- Higher impact in summer than in winter.



The high frequency part of the wave spectrum is characterized by discrete bands!

Strong seasonality in western boundary currents due to submesoscales: Results have been confirmed in the Gulf Stream by experimental data [Oleander, LatMix] (Callies et al., NC'15)

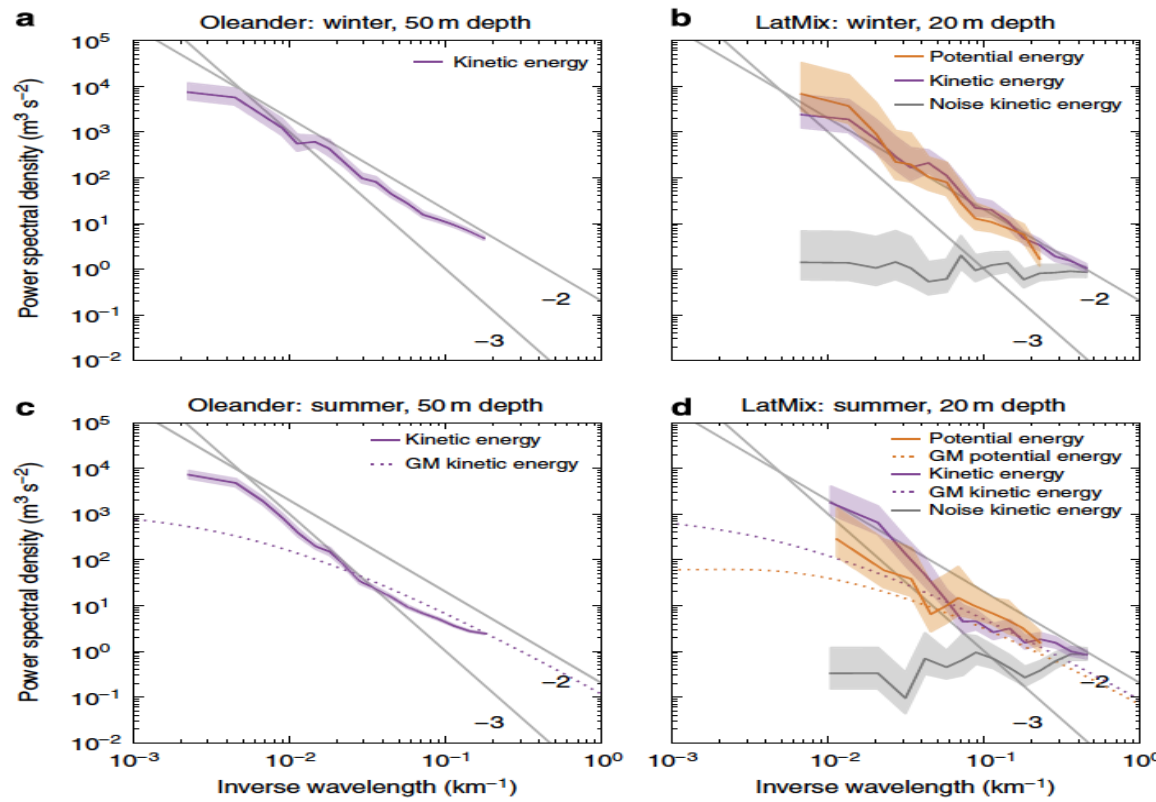


Figure 3 | Seasonality in observations. (a) Kinetic energy spectrum at 50 m depth for the Oleander winter data. (b) Potential and kinetic energy spectra at 20 m depth for the LatMix winter experiment. (c) Kinetic energy spectrum at 50 m depth for the Oleander summer data. (d) Potential and kinetic energy spectra at 20 m depth for the LatMix summer experiment. The light shadings are 95% confidence intervals. Also shown are the GM model spectra for internal waves in the seasonal thermocline (with parameters from ref. 30), estimates for the noise level of the LatMix velocity data and reference lines with slopes -2 and -3 .

Internal waves affect the velocity spectrum at scales < 50-100 km in summer
See also Callies et al. JPO 2013, Qiu et al. 2016 in press

THE INTERNAL WAVE FIELD IS INTENSIFIED AT SMALL SCALES

Time in days: 0.00

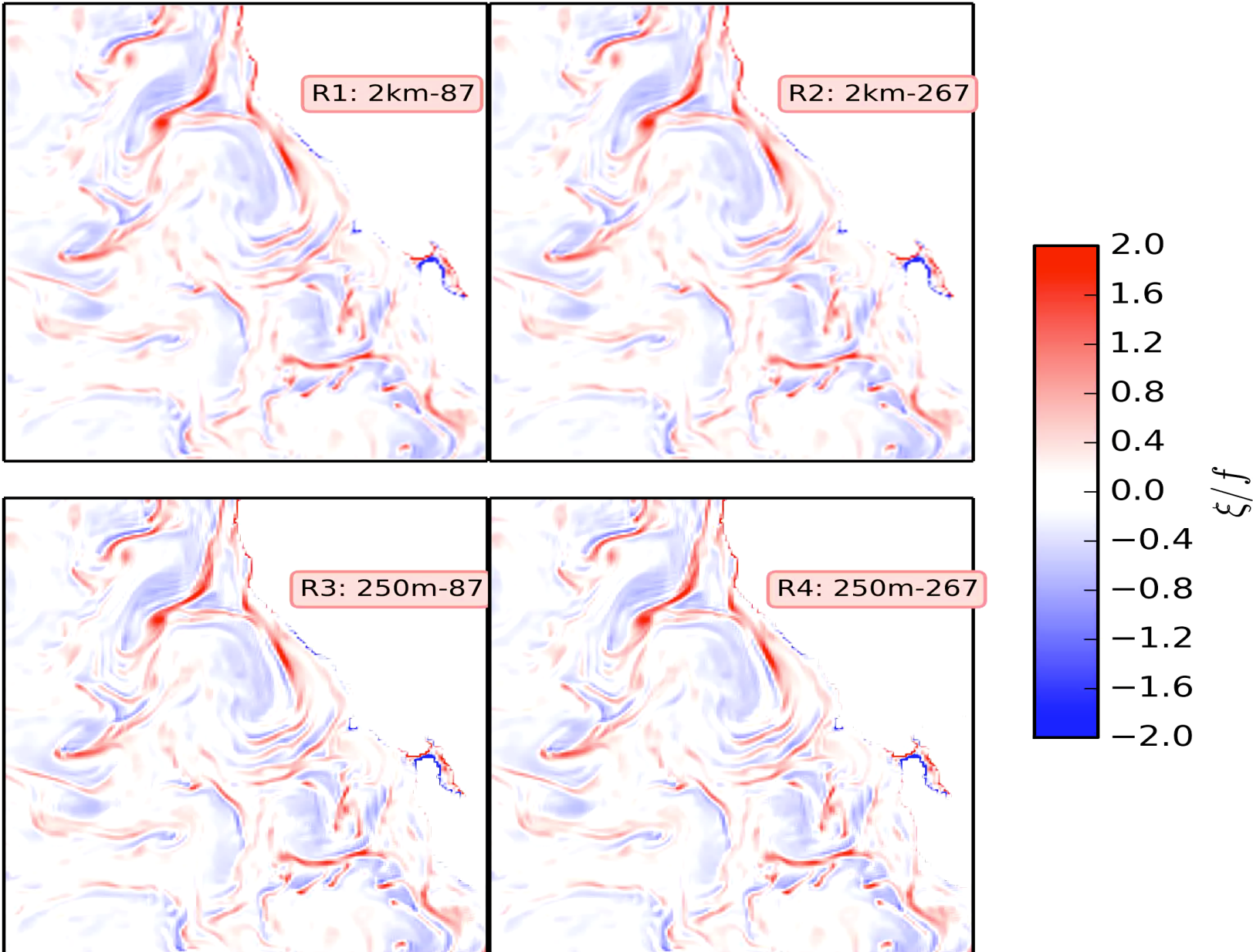
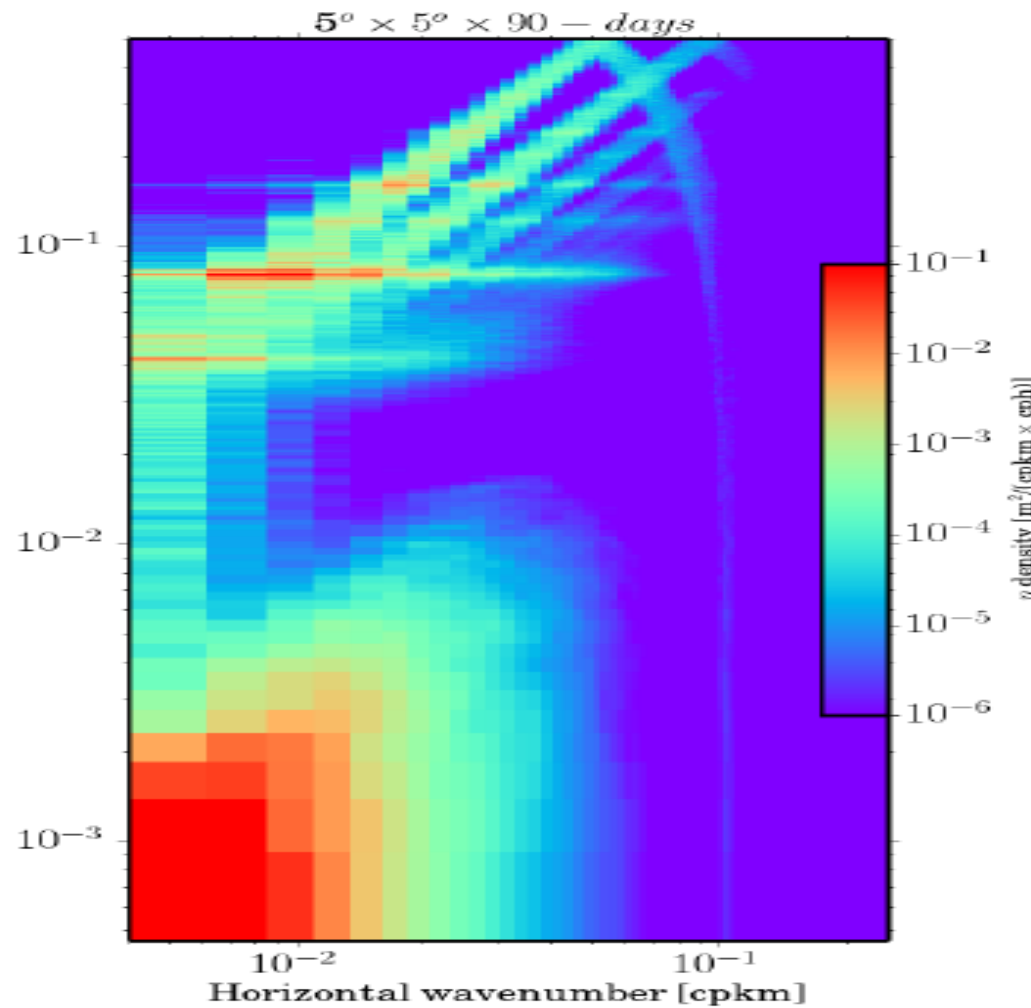


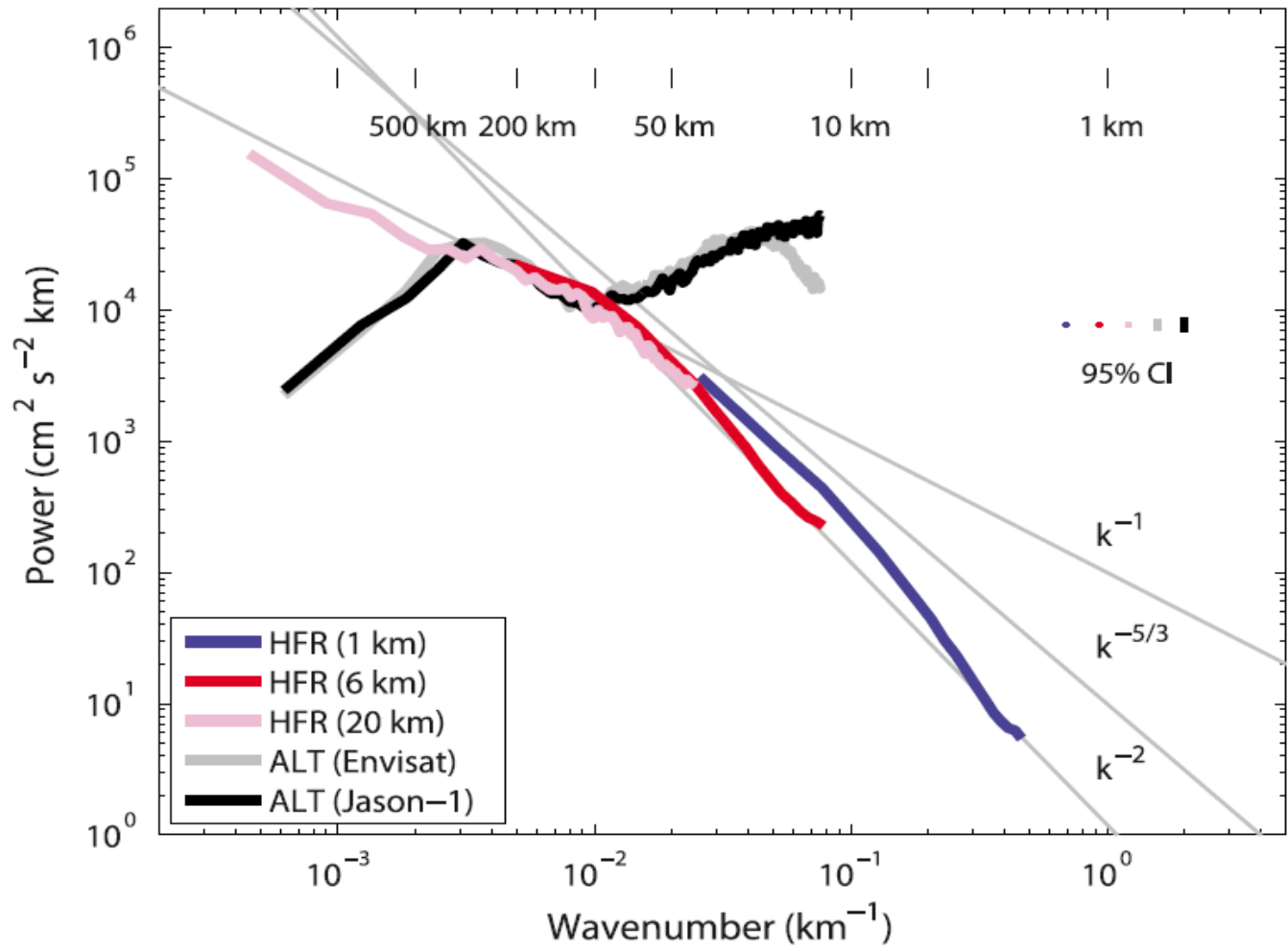
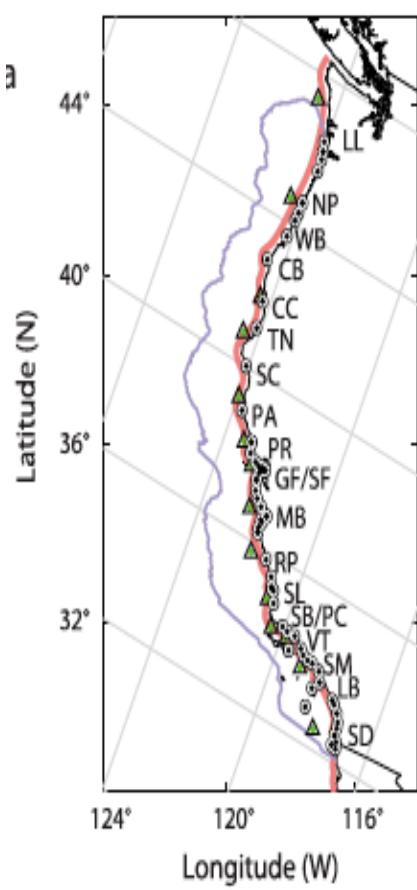


Figure 1. RADARSAT SAR image of the Santa Barbara Channel at 1400 UT on January 8, 2003. The area is 100 km by 110 km. The image was provided by B. Holt, Jet Propulsion Laboratory, and processed at the Alaska Satellite Facility. (Copyright by the Canadian Space Agency (2003)).

CAN WE GET A FREQUENCY-WAVENUMBER SPECTRUM FROM OBSERVATIONS ?

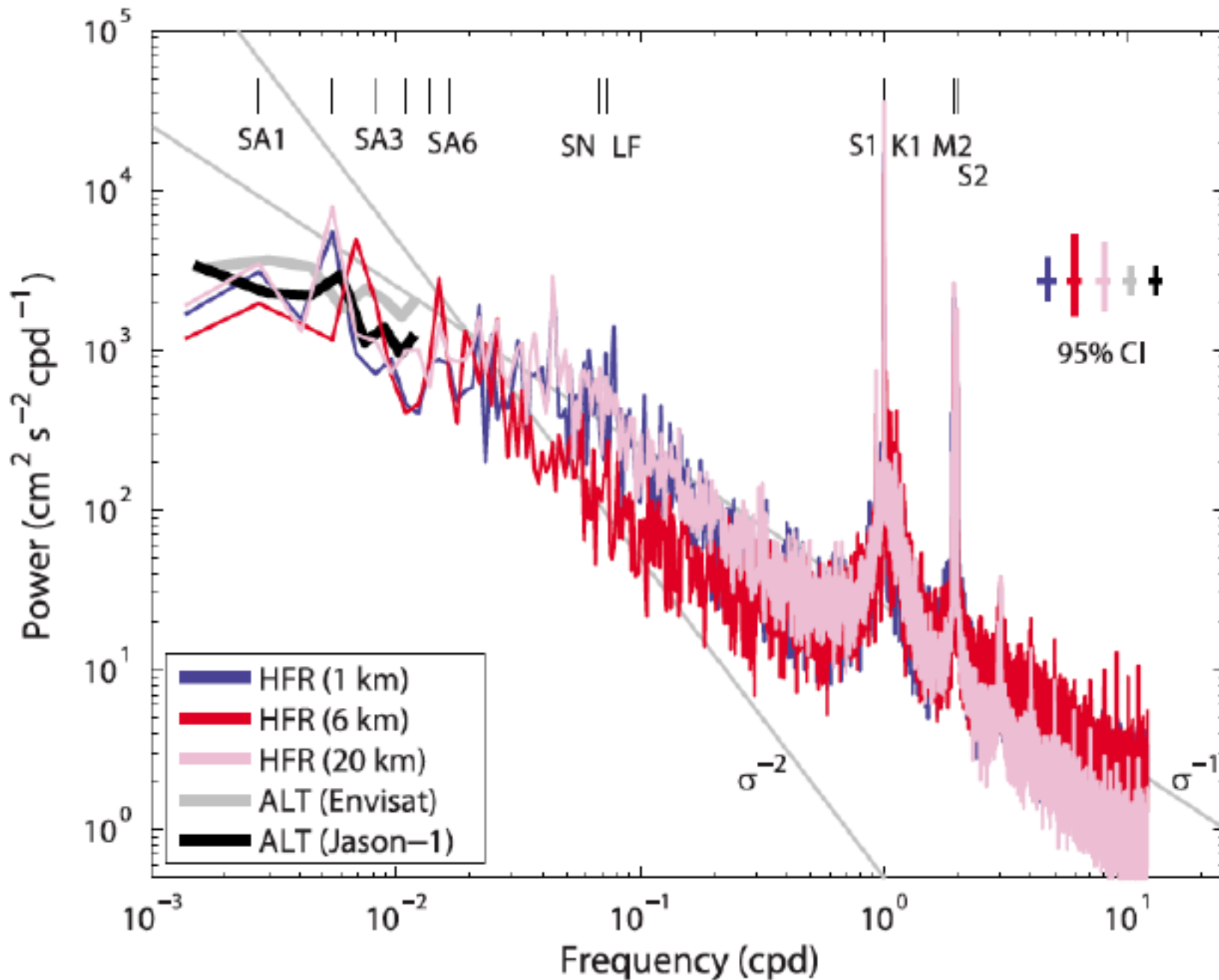


HIGH-FREQUENCY RADAR OBSERVATIONS MAY HELP ...



Kim et al.,'11, using **HF radar observations**, indicate that the velocity spectrum (NE Pacific) is in k^{-2} , in particular in the range of submesoscales

b



WAVE SPECTRUM:

- WHY THESE DISCRETE KE BANDS ?
- WHY A SEASONALITY ENHANCED IN SUMMER ?
- SINCE WAVE FORCINGS ARE LARGE-SCALE, WHAT PRODUCES WAVES AT SMALL SCALES?

Waves in a stratified and rotating flow

We assume the flow is hydrostatic at first order, $R_{\text{ol}} \ll 1$ (nonlinear terms are negligible), and $1/fT = O(1)$. The resulting equations are:

$$\frac{\partial u}{\partial t} - fv = -\frac{1}{\rho_0} \frac{\partial p'}{\partial x}$$

$$\frac{\partial v}{\partial t} + fu = -\frac{1}{\rho_0} \frac{\partial p'}{\partial y}$$

$$0 = -\frac{1}{\rho_0} \frac{\partial p'}{\partial z} - \frac{g}{\rho_0} \rho'$$

$$\frac{\partial u}{\partial x} + \frac{\partial v}{\partial y} + \frac{\partial w}{\partial z} = 0$$

$$\frac{\partial \rho'}{\partial t} + w \frac{d\bar{\rho}}{dz} = 0.$$

Let us find the equation for p' ...

We use $N^2(z) = -\frac{g}{\rho_0} \frac{d\bar{\rho}}{dz} > f^2 > 0$.

This leads to:

$$\frac{\partial}{\partial t} \left[\left(\frac{p'_z}{N^2} \right)_{ztt} + f^2 \left(\frac{p'_z}{N^2} \right)_z + \Delta p' \right] = 0$$

1 – let us assume $N^2 = \text{cst}$

$$\Rightarrow \frac{\partial}{\partial t} [p'_{zztt} + f^2 p'_{zz} + N^2 \Delta p'] = 0$$

Boundary conditions:

$$W=0, \quad \text{at } z=0, -H$$

which leads to: $\frac{\partial \rho'}{\partial t} = 0$ and therefore $\frac{\partial p'}{\partial z} = 0$ at $z=0, -H$

Using $p'(x, y, z, t) = P(z) e^{-i(k.x + l.y - \omega t)}$, leads to

$$P_{zz} - \frac{k^2 + l^2}{f^2 - \omega^2} N^2 P = 0$$

Using $n'(x, y, z, t) = \cos mz e^{-i(k.x + l.y - \omega t)}$ leads to the dispersion relation:

Using $p'(x,y,z,t) = P(z).e^{-i(k.x+l.y-\omega t)}$, leads to

$$P_{zz} - \frac{k^2 + l^2}{f^2 - \omega^2} N^2 P = 0$$

P can be decomposed in a Fourier series that satisfies the BCs;

Using $P(z) = \cos mz$ leads to the dispersion relation:

$$\omega^2 = f^2 + N^2 \frac{k^2 + l^2}{m^2}$$

ω^2 depends on the angle between $K = \sqrt{k^2 + l^2}$ and m

- Strong similitudes between the SW system and the equations for p' and ω^2 ...
[$C_o^2 = gH$ is replaced by N^2/m^2 , but m can vary since several vertical scales are allowed].
- Note that N^2/f^2m^2 is the equivalent of L_d^2 (see before) as gH/f^2 was called R^2
- $Bu = N^2K^2/f^2m^2 = L_d^2/L^2$ is also called the Burger number

2 – let us assume $N^2 = N^2(z)$:

This leads to:

$$\frac{\partial}{\partial t} \left[\left(\frac{p'_z}{N^2} \right)_{ztt} + f^2 \left(\frac{p'_z}{N^2} \right)_z + \Delta p' \right] = 0$$

Using $p'(x,y,z,t) = P(z) \cdot e^{-i(k.x+l.y-\omega t)}$, leads to

$$\left(\frac{P_z}{N^2} \right)_z - \frac{k^2 + l^2}{f^2 - \omega^2} P = 0$$

We need to find new vertical normal modes for $P(z)$ (cosines do not work anymore since $N^2 = N^2(z)$).

These vertical normal modes, $F_m(z)$, should be such that $\int_{-H}^0 F_m \cdot F_n \, dz = \delta_{mn}$.

Then we can use $P(z) = \sum_{m=1}^M P_m \cdot F_m(z)$

Vertical dimension using normal modes:

Normal modes are obtained by solving the Sturm-Liouville equation (after [J. Sturm](#) (1803–1855) and [J. Liouville](#) (1809–1882)):

$$\frac{d}{dz} \frac{f^2}{N^2} \frac{dF_m}{dz} = - \lambda_m^2 F_m.$$

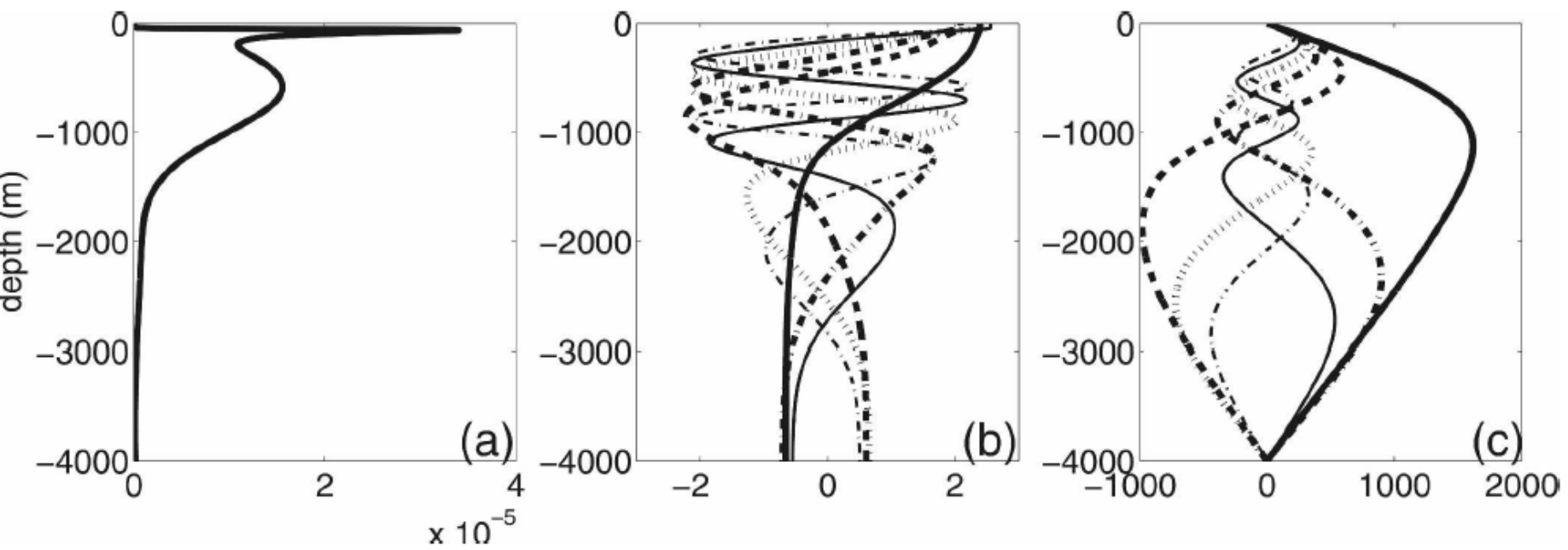
with $dF_m/dz = 0$ at $z=0, -H$.

F_m is the eigenfunction and λ_m^2 the eigenvalue (or the vertical wavenumber) associated with mode m .

Modes are orthonormal :

$$\int_{-H}^0 F_m \cdot F_n dz = \delta_{mn}$$

with $\lambda_m = 1/r_m$. r_m is also called the Rossby radius of deformation of mode m



1. (a) Vertical profiles of N^2 , (b) the first six eigenfunctions F_n given by Eq. (3), and (c) the first six functions H_n . Units in (a) are s^{-2} .

$$\mathcal{L}F_n = -\frac{1}{r_n^2} F_n \quad \mathcal{L}(\cdot) = \frac{\partial}{\partial z} \left[\frac{f^2}{N^2} \frac{\partial}{\partial z} (\cdot) \right]$$

$$H_n(z) = \int_z^0 F_n(z') dz'$$

This leads to the following dispersion relation:

$$\omega^2 = f^2 + f^2 r_m^2 [k^2 + l^2]$$

$f.r_m$ is the equivalent of c_o of the SW system and r_m is the Rossby radius of deformation ($\sim L_d$) of mode m (the equivalent of $c_o/f=R$ in the SW system).

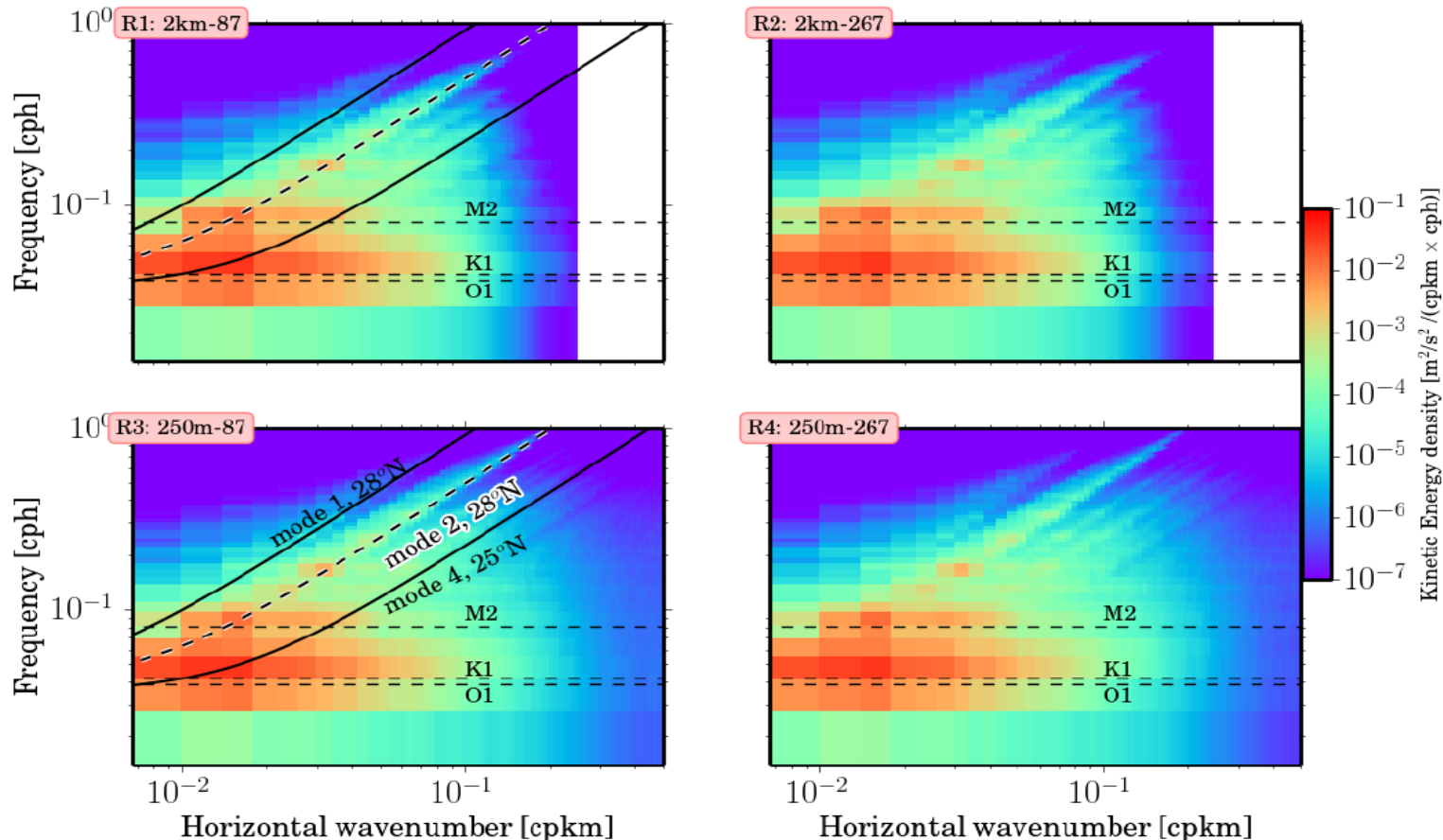
Solutions of the linear equations are Poincaré waves, with

- inertial waves as the long wave limit with $L \gg r_m$ ($Bu \ll 1$) and
- gravity waves as the short limit when $L \ll r_m$ ($Bu \gg 1$).
- Kelvin waves exist as well.

Since the vertical normal modes have different phase speeds for the same $K^2 = k^2 + l^2$, vertical modes, if initially in phase, quickly become out of phase, leading to the vertical propagation of the kinetic energy (see Gill, JPO'84, next class).

Kinetic energy associated with linear Poincaré waves well emerge in HR numerical simulations.

This explains the discrete bands in the $\omega - k$ spectrum



Using $p'(x,y,z,t) = P(z).e^{-i(k.x+l.y-\omega t)}$, leads to

$$P_{zz} - \frac{k^2 + l^2}{f^2 - \omega^2} N^2 P = 0$$

P can be decomposed in a Fourier series that satisfies the BCs;

Using $P(z) = \cos mz$ leads to the dispersion relation:

$$\omega^2 = f^2 + N^2 \frac{k^2 + l^2}{m^2}$$

ω^2 depends on the angle between $K = \sqrt{k^2 + l^2}$ and m

- Strong similitudes between the SW system and the equations for p' and ω^2 ...
[$C_o^2 = gH$ is replaced by N^2/m^2 , but m can vary since several vertical scales are allowed].
- Note that N^2/f^2m^2 is the equivalent of L_d^2 (see before) as gH/f^2 was called R^2
- $Bu = N^2K^2/f^2m^2 = L_d^2/L^2$ is also called the Burger number

GROUP VELOCITY:

$$C_{gx} = \frac{N^2 k}{\omega m^2}$$

$$C_{gy} = \frac{N^2 l}{\omega m^2}$$

$$C_{gz} = -\frac{N^2(k^2 + l^2)}{\omega m^3} \quad (\text{downward propagation if } \omega > 0)$$

Note that: $\vec{C}_g \cdot \vec{K} = 0$!

Example:

$N=6.10^{-3}$, $L=80\text{km}$, $H=350\text{m}$, $\omega = 1.03f$, leads to $C_{gz} = 80\text{m.d}^{-1}$

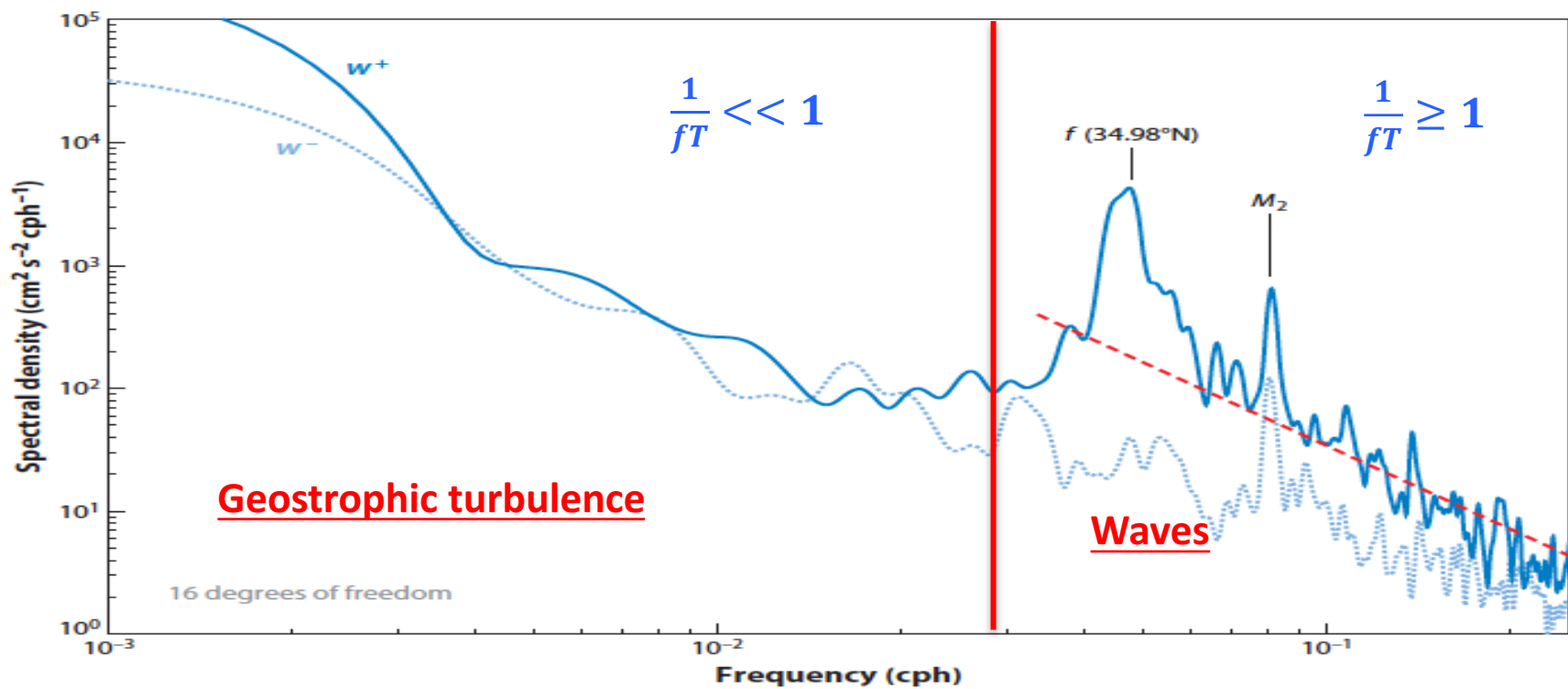


Figure 1

Rotary velocity spectrum at 261-m depth from current-meter data from the WHOI699 mooring gathered during the WESTPAC1 experiment (mooring at 6,149-m depth.) The solid blue line (w^+) is clockwise motion, and the dashed blue line (w^-) is counterclockwise motion; the differences between these emphasize the downward energy propagation that often dominates the near-inertial band. The dashed red line is the line $E_0 N \omega^{-p}$ with $N = 2.0$ cycles per hour (cph), $E_0 = 0.096 \text{ cm}^2 \text{ s}^{-2} \text{ cph}^{-2}$, and $p = 2.25$, which is quantitatively similar to levels in the Cartesian spectra presented by Fu (1981) for station 5 of the Polygon Mid-Ocean Experiment (POLYMODE) II array.

A frequency spectrum displays different properties between fast and slow motions

INTERNAL WAVE ENERGY IS PROPAGATING DOWNWARD (why? see next classes)

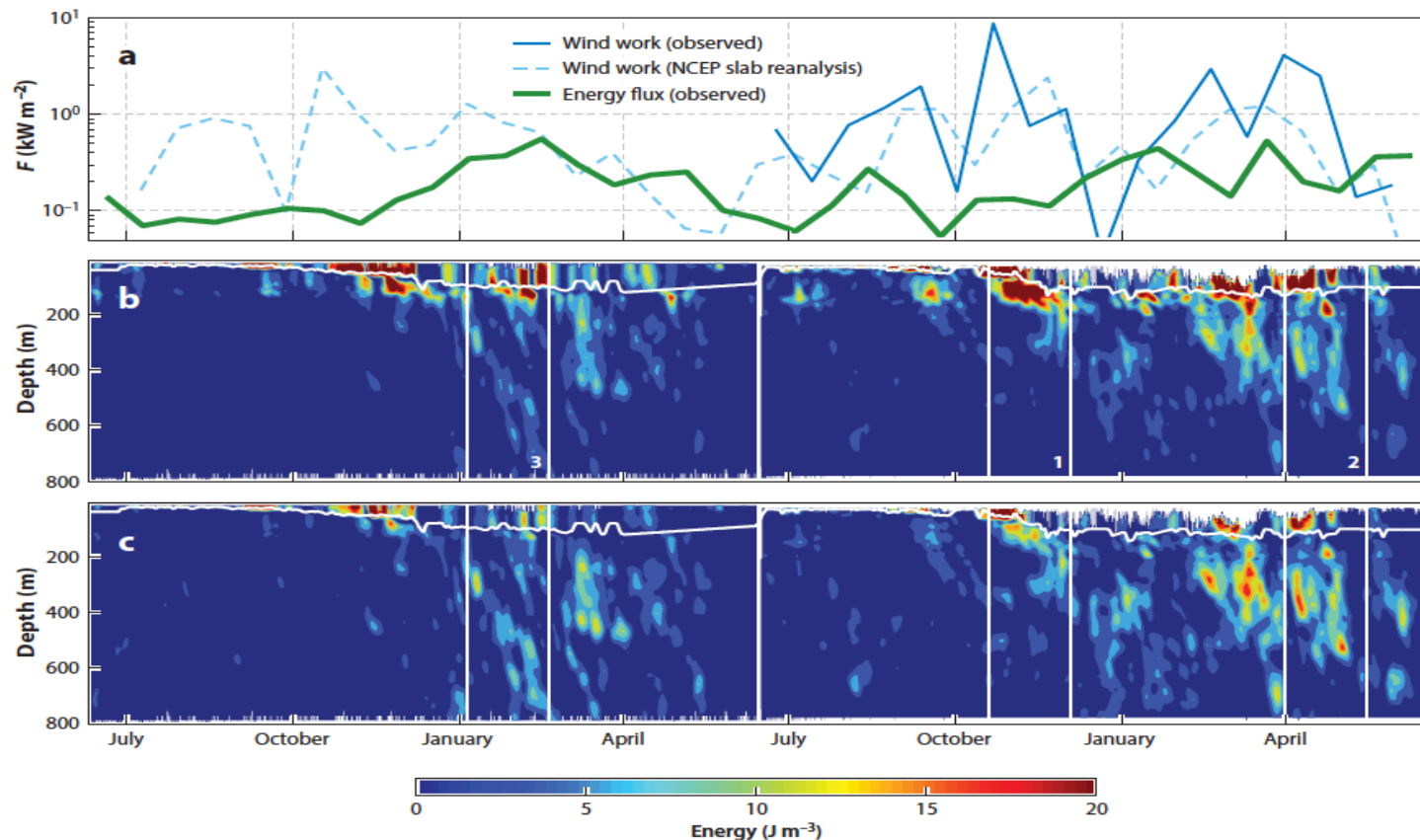


Figure 5

Near-inertial waves at Ocean Station Papa. (a) Wind work from observations (solid blue line) and from Equation 2 forced with reanalysis winds (dashed blue line), along with observed energy flux computed as the mean of energy from 600 to 800 m multiplied by $c_{gz} = 1.03 \times 10^{-4} \text{ m s}^{-1}$ (9 m d^{-1} ; thick green line). All three lines have been smoothed over 20 days. (b) Near-inertial kinetic energy for the whole two-year record. (c) The same as panel b but additionally accounting for WKB refraction. In panels b and c, the mixed-layer depth is overplotted in white. Abbreviations: NCEP, National Centers for Environmental Prediction; WKB, Wentzel, Kramers, Brillouin. Modified from Alford et al. (2012).

Next class: vertical propagation of wave energy using the vertical normal modes: How it works ...